Graphene Oxide Derivatives

Matrix-assisted laser desorption/ionization (MALDI) has been considered as one of the most powerful analytical tools for mass spectrometry (MS) analysis of large molecular weight compounds such as proteins, nucleic acids, and synthetic polymers thanks to its high sensitivity, high resolution, and compatibility with high-throughput analysis. Despite these advantages, MALDI cannot be applied to MS analysis of small molecular weight compounds (<500 Da) because of the matrix interference in low mass region. Therefore, numerous efforts have been devoted to solving this issue by using metal, semiconductor, and carbon nanomaterials for MALDI time-of-flight MS (MALDI-TOF-MS) analysis instead of organic matrices. Among those nanomaterials, graphene oxide (GO) is of particular interest considering its unique and highly tunable chemical structures composed of the segregated sp^2 carbon domains surrounded by sp^3 carbon matrix.

1. Introduction

Matrix-assisted laser desorption/ionization (MALDI) technique, often combined with time-of-flight mass spectrometry (MALDI-TOF-MS), has been considered as a powerful and essential technique to analyze the intact molecular weight of high-molecular-weight compounds such as proteins [1], nucleic acids [2] and synthetic polymers [3] without their undesired fragmentation. This soft-ionization strategy has significantly contributed to the advances in chemical and biological researches based on its simple analysis process, miniscule sample consumption, high resolution, salt-tolerance, sensitivity and compatibility with high-throughput analysis [4][5]. The detailed mechanism of the MALDI process is still not fully understood, but it has been generally described by serial 3-step processes including laser energy transfer from matrix to analyte in their solid-state mixture upon laser irradiation, ionization by photochemical reaction and isolation of ionized analyte in excess matrix for mass spectrometric analysis [4]. Although MALDI-TOF-MS has been successfully applied to biological and polymer research fields for the molecular weight analysis of high-molecular-weight compounds, it cannot be directly harnessed to analyze low-molecular-weight compounds owing to the severe background interference in the low-mass region from detector saturation and/or photochemical side reactions by organic matrices such as 2,5-dihydroxybenzoic acid (DHB), α-cyano-4-hydroxycinnamic acid (CHCA), sinapic acid, and caffeic acid [6]. For addressing this issue, many efforts have been devoted to the development of an efficient alternative to organic matrices that can be used in matrix-free laser desorption/ionization time-of-flight mass spectrometry (LDI-TOF-MS) [7][8][9]. Metal [10], semiconductor [11][12][13][14], and carbon nanomaterials [15][16][17][18] have been extensively investigated as potential mediators for the LDI-TOF-MS analysis of important low-molecular-weight compounds, including amino acids, saccharides, lipids, organic pollutants, and small peptides. The laser desorption/ionization (LDI) efficiency of those nanomaterials significantly depends on their chemical composition, size and morphology [12][19]. Therefore, development of an efficient nanomaterials-based LDI-TOF-MS platform for the analysis of those small molecules has been of central interest and has attracted much research attention from the material scientists [8]. Based on those efforts, important requirements, such as high surface area, colloidal stability, laser absorption capacity, electrical and thermal conductivity and photo-thermal conversion property, have been revealed to fabricate an efficient platform for LDI-TOF-MS analysis [20][21]. In addition to those colloidal nanomaterials, various nanoporous substrates including porous silicon [22] and titania [23] have also been investigated as a chip-based analytical platform for LDI-TOF-MS analysis of small molecules. Especially, porous silicon substrates are recognized as one of the representative chip-based LDI-TOF-MS platforms because of their excellent LDI efficiency derived from the high surface area, amenable surface and uniform mass signal distribution [24][25]. The efficiency of those nanoporous substrates in LDI-TOF-MS analysis has also been enhanced by surface modification [26][27] and subsequent nanohybridization with other functional nanomaterials [28][29].

Among those various materials, carbon nanomaterials such as graphene [30][31][32][33], mesoporous carbon [34], graphene oxide (GO) [35], carbon nanotube (CNT) [36], and carbon dot (CD) [16][37] have been considered as excellent candidates because they meet most of the requirements as an efficient mediator for LDI-TOF-MS analysis of small molecules. In addition to the general requirements, the carbon materials can provide cost-effectiveness, functionalizable surface and

strong affinity to various biomolecules [38] and environmental pollutants [39][40][41]. Especially, GO is a distinct carbon nanomaterial owing to its unique chemical structures composed of small segregated sp^2 carbon domain surrounded by sp^3 carbon matrix presenting oxygen containing functional groups [42]. Those sp^2 carbon structures of GO derivatives play an important role in LDI-TOF-MS analysis by absorbing laser energy and converting it into thermal energy through the electron-phonon interaction for LDI of small molecules [35]. In this regard, Raman spectroscopy is a powerful and essential analytical tool to characterize the ordered and defected sp^2 carbon structures of GO derivatives and their nanohybrid structures, which are closely related to their electron-phonon transition and then their efficiency in LDI-TOF-MS analysis [42][43][44]. GO derivatives are a complex family presenting the structural diversity depending on their synthetic and post-treatment processes. The physicochemical properties of GO derivatives greatly affect their behavior in LDI-TOF-MS analysis, and their detailed chemistry has been extensively reviewed elsewhere [45][46][47][48][49][50][51][52]. In addition, GO can be converted into graphene analogues by chemical and thermal reduction treatments for partial removal of oxygen containing functional groups, mainly hydroxyl and epoxy groups. However, there still remains residual oxygen containing functional groups on the reduced GO (RGO) because of the restricted degree of deoxygenation [52]. Thanks to these residual oxygen containing functional groups, GO and RGO derivatives can be hybridized with metal, metal oxide, and semiconductor nanomaterials by covalent and non-covalent surface modifications. The resulting nanohybrid structures can enrich thioloated, phosphorylated and/or aromatic biomolecules such as nucleic acids, amino acids, peptides and proteins through metal-thiol, metal oxide-phosphate and π-π interactions, respectively [53][54][55][56]. Based on those properties, GO and RGO derivatives and their nanohybrid structures have been actively investigated for LDI-TOF-MS analysis and exhibited a strong and versatile potential to analyze various kinds of important small molecules. There are several review articles which deal with the various nanomaterials-based matrices for LDI-TOF-MS analysis of small molecules [19].

2. GO Derivatives for LDI-TOF-MS Analysis

Dong et al. [57] reported that graphene can be harnessed as a novel matrix for LDI-TOF-MS analysis of various small molecules, such as amino acids, polyamines, anticancer drugs, nucleosides and steroids, regardless of their polarity. It is noteworthy that the graphene used in this report was actually chemically-RGO flakes. Although the term graphene is only applicable to a single-layer of networked atomic sp^2 carbon sheet compacted into a honeycomb lattice, it has been widely misused for RGO and few-layered graphite [58][59]. Therefore, we will use the term "RGO" rather than "graphene" throughout this review because most of the cited literature have utilized RGO for LDI-TOF-MS analysis of small molecules. In the report of Dong et Al., RGO was synthesized by using sodium dodecylbenzene sulfonate (SDBS) as a surfactant to prevent irreversible aggregation of RGO in aqueous media through the van der Waals and π-π interactions between their basal planes [60]. Despite of the surface-adsorbed SDBS on RGO, the resulting RGO exhibited many advantages for LDI-TOF-MS analysis of small molecules such as the high reproducibility, salt tolerance and applicability to the solid-phase extraction of squalene [57]. This report presents the possibility of GO derivatives as an efficient platform for LDI-TOF-MS analysis. However, it is of note that the surfactants on GO derivatives can interfere with the efficient energy transfer to analytes and solid-phase extraction, and thus the follow-up studies are generally excluded to use surfactants to prepare GO derivatives and their nanohybrid structures.

To address this issue, Zhou et al. [61] developed a RGO films-based LDI-TOF-MS platform by sequential fabrication processes including spin-coating of GO and subsequent chemical reduction by using hydrazine vapor. In this case, the RGO sheets were stably immobilized on a solid substrate and thus there was no demand of surfactants for dispersion in solvents. The resulting RGO films showed a higher efficiency and better reproducibility for LDI-TOF-MS analysis of an environmental pollutant, octachlorodibenzo-p-dioxin (OCDD), than the dispersed RGO powder. The limit of detection (LOD) of OCDD was found to be 500 pg with RGO films and the obtained signal was higher than the RGO powder. This difference was attributed to the clean surface of RGO films, and their planar and well-interconnected structures which facilitate the π-π interaction with OCDD, laser energy absorption, and energy transfer to OCDD for LDI-TOF-MS analysis. This report clearly shows that the advantages of chip-based LDI-TOF-MS platform.

Lu et al. [62] demonstrated that the efficiency of RGO flakes in LDI-TOF-MS analysis was higher under negative ionization mode than positive ionization mode. Based on their results, the mass spectra of peptides, amino acids, fatty acids, nucleosides and nucleotides can be obtained by using RGO flakes under both positive and negative ionization modes, but there was a clear difference in mass spectra obtained under positive and negative ionization modes. The mass spectra obtained under positive ionization mode were composed of many kinds of multiple cationic adducts with proton and alkali metals such as $[M + H]^+$, $[M + Na]^+$, $[M + K]^+$, $[M + 2Na - H]^+$ and $[M + Na + K - H]^+$. By stark contrast, the mass spectra obtained under a negative ionization mode were only composed of a single deprotonated form such as $[M - H]^-$. Since the formation of multiple adducts makes identification of analytes complicated, the applicability of RGO flakes to a negative ionization mode facilitates its wide-spread usage for LDI-TOF-MS analysis [30][37][62].

The size and structure of graphene derivatives might also have significant influence on the LDI-TOF-MS analysis. Liu et al. [63] investigated the LDI efficiency of graphene derivatives such as graphene, GO and RGO for LDI-TOF-MS analysis of small molecules under negative ionization mode. According to the results, the graphene prepared by chemical vapor deposition showed no activity as a matrix for LDI-TOF-MS analysis, but GO and RGO flakes presented a high efficiency for LDI-TOF-MS analysis of flavonoids and coumarin derivatives. Interestingly, the LDI efficiency of GO flakes was much higher than that of RGO flakes even at 1 pmol of flavonoids, which is presumably attributed to the abundant carboxylic acid groups on GO flakes. The authors also explored size effect of GO flakes on LDI-TOF-MS analysis and found that millimeter-sized GO flakes provide a higher LDI efficiency than micrometer-sized GO flakes for the analysis of flavonoids [63].

Kim et al. [64] investigated the size influence of GO flakes on their fragmentation behavior during LDI-TOF-MS analysis of small molecules (Figure 1a). Considering that the fragmentation of GO flakes mainly occurs on the defect sites and labile structures composed of epoxide groups, the fragmentation of GO flakes can be strongly dependent on their lateral dimension [64]. The GO flake larger than 5 μm in their lateral dimension underwent severe fragmentation compared to the GO flakes smaller than 1 μm (Figure 1b). This observation was attributed to the increased density of defects and epoxide groups on the basal plane GO flakes with their lateral dimension [65]. The results implied that the smaller GO flakes lead to the less fragmentation during LDI-TOF-MS analysis, and this hypothesis was further confirmed with LDI-TOF-MS analysis by using nano-sized GO (NGO) flakes which obtained clear mass spectra of small molecules without interference from the fragmentation of GO flakes in low mass region [64]. By using NGO as a matrix, organic pollutants such as benzoyldibenzo-p-dioxin (BDPD), benzo[a]pyrene (B[a]P), and perfluorobutyric acid (PBA) were analyzed with LDI-TOF-MS and the LOD was determined as 15 fg, 150 fg, and 15 pg, respectively. Overall, these outcomes clearly show the potential of LDI-TOF-MS analysis to be directly utilized for investigating the chemical structure of GO derivatives.
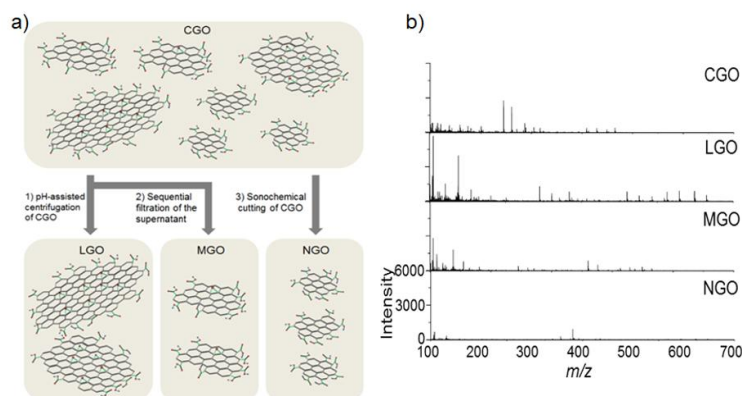

Figure 1. (**a**) A schematic diagram of size-fractionalization of GO flakes depending on their lateral of dimension. (**b**) LDI-TOF-MS spectra of small molecules obtained by using size-fractionalized GO flakes. Adapted with permission from ref. [64]. Copyright 2015 Wiley-VCH.

The origin of the fragmentation behavior of GO derivatives in LDI-TOF-MS analysis was further investigated [66][67], as the true structure of GO sheets is debated owing to the recent discovery of highly oxidized species present on their surface [68]. The origin of the fragmentation could be traced to the direct fragmentation of a core graphene-like sheet or the detachment of the surface-adsorbed oxidative debris (OD). To determine the source of fragmentation, a graphene-like sheet and OD were separated from as-synthesized GO (aGO) through a base-washing process (Figure 2a), and the resulting graphene-like sheet (bwGO) and OD were subjected to LDI-TOF-MS analysis under identical conditions (Figure 2b). Comparison of LDI-TOF-MS spectra of bwGO to that of aGO showed that aGO exhibited mass peaks attributed to both pure and oxidized carbon clusters, while bwGO presented much stronger mass peaks solely due to the pure carbon clusters (Figure 2c). These results indicate that the fragmentation of GO sheets originates from both the core graphene-like sheet and the detachment of the surface-adsorbed OD; however, the separation process leads to the partial reduction of these GO sheet constituents.
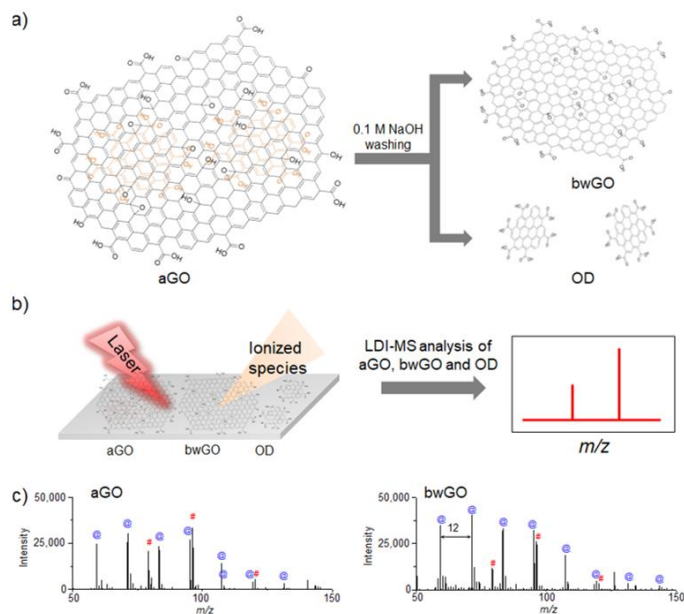
Figure 2. Schematic diagrams of (**a**) the separation process of OD and bwGO from aGO by washing with 0.1 M NaOH, and (**b**) LDI-TOF-MS analysis process of the obtained aGO and bwGO. (**c**) LDI-TOF-MS spectra of aGO and bwGO, The symbol @ in blue color corresponds to the carbon cluster ions and the symbol # in red color corresponds to the oxidized carbon cluster ions. Adapted from ref. [66] with permission from The Royal Society of Chemistry.

In addition, the influence of OD on the efficiency of LDI-TOF-MS analysis was further investigated by comparing aGO and bwGO. The efficiency of the LDI-TOF-MS analysis of various analytes, was higher with bwGO than with aGO regardless of their chemical structure and molecular weight (Figure 3). The LOD of small molecules with bwGO was determined to be approximately 10 pmol which is lower than that with aGO (100 pmol). This demonstrates that the photo-thermal conversion efficiency of GO derivatives can be enhanced simply by removing the surface-adsorbed OD [67].
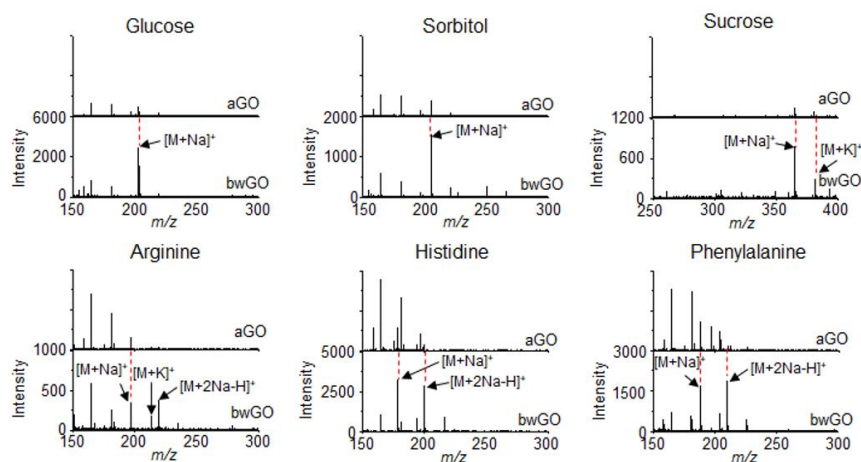

Figure 3. LDI-TOF-MS spectra of small molecules such as glucose, sorbitol, sucrose, arginine, histidine, and phenylalanine obtained with aGO and bwGO. Reproduced with permission from ref. [67]. Copyright (2019) Japan Society for Analytical Chemistry.

References

1. Liu, T.; Belov, M.E.; Jaitly, N.; Qian, W.J.; Smith, R.D. Accurate mass measurements in proteomics. Rev. 2007, 107, 3621–3653, doi:10.1021/cr068288j.

2. Gao, X.; Tan, H.; Sugrue, R.J.; Tang, K. MALDI mass spectrometry for nucleic acid analysis. Top. Curr. Chem. 2013, 331, 55–77, doi:10.1007/128_2012_366.

3. Hyzak, L.; Moos, R.; Von Rath, F.; Wulf, V.; Wirtz, M.; Melchior, D.; Kling, H.W.; Köhler, M.; Gäb, S.; Schmitz, O.J. Quantitative matrix-assisted laser desorption ionization-time-of-flight mass spectrometry analysis of synthetic polymers and peptides. Chem. 2011, 83, 9467–9471, doi:10.1021/ac2021739.

4. Karas, M.; Bahr, U.; Giessmann, U. Matrix-assisted laser desorption ionization mass spectrometry. Mass Spectrom. Rev. 1991, 10, 335–357.

5. Aebersold, R.; Goodlett, D.R. Mass spectrometry in proteomics. Rev. 2001, 101, 269–295, doi:10.1021/cr990076h.

6. Guo, Z.; Zhang, Q.; Zou, H.; Guo, B.; Ni, J. A method for the analysis of low-mass molecules by MALDI-TOF mass spectrometry. Chem. 2002, 74, 1637–1641, doi:10.1021/ac010979m.

7. Silina, Y.E.; Volmer, D.A. Nanostructured solid substrates for efficient laser desorption/ionization mass spectrometry (LDI-MS) of low molecular weight compounds. Analyst 2013, 138, 7053–7065, doi:10.1039/c3an01120h.

8. Chiang, C.K.; Chen, W.T.; Chang, H.T. Nanoparticle-based mass spectrometry for the analysis of biomolecules. Soc. Rev. 2011, 40, 1269–1281, doi:10.1039/c0cs00050g.

9. Kawasaki, H.; Sugitani, T.; Watanabe, T.; Yonezawa, T.; Moriwaki, H.; Arakawa, R. Layer-by-layer self-assembled mutilayer films of gold nanoparticles for surface-assisted laser desorption/ionization mass spectrometry. Chem. 2008, 80, 7524–7533, doi:10.1021/ac800789t.

10. McLean, J.A.; Stumpo, K.A.; Russel, D.H. Size-selected (2–10 nm) gold nanoparticles for matrix assisted laser desorption ionization of peptides. Am. Chem. Soc. 2005, 127, 5304–5305, doi:10.1021/ja043907w.

11. Brodoceanu, ; Elnathan, R.; Prieto-Simón, B.; Delalat, B.; Guinan, T.; Kroner, E.; Voelcker, N.H.; Kraus, T. Dense arrays of uniform submicron pores in silicon and their applications. ACS Appl. Mater. Interfaces 2015, 7, 1160–1169, doi:10.1021/am506891d.

12. Zhu, ; Wang, Z.; Wang, Y.; Teng, F.; Du, J.; Dou, S.; Lu, N. Investigation of surface morphology on ion desorption in SALDI-MS on tailored silicon nanopillar arrays. J. Phys. Chem. C 2020, 124, 2450–2457, doi:10.1021/acs.jpcc.9b09520.

13. Zhu, Q.; Teng, F.; Wang, Z.; Wang, Y.; Lu, N. Confining analyte droplets on visible Si pillars for improbing reproducibility and sensitivity of SALDI-TOF MS. Bioanal. Chem. 2019, 411, 1135–1142, doi:10.1007/s00216-018-01565-5.

14. Wang, X.; Teng, F.; Wang, Y.; Lu, N. Rapid liquid-phase microextraction of analytes from complex samples on superwetting porous silicon for onsite SALDI-MS analysis. Talanta 2019, 198, 63–70, doi:10.1016/j.talanta.2019.01.051.

15. Rainer, M.; Qureshi, M.N.; Bonn, G.K. Matrix-free and material-enhanced laser desorption/ionization mass spectrometry for the analysis of low molecular weight compounds. Bioanal. Chem. 2011, 400, 2281–2288, doi:10.1007/s00216-010-4138-1.

16. Chen, S.; Zheng, H.; Wang, J.; Hou, J.; He, Q.; Liu, H.; Xiong, C.; Kong, X.; Nie, Z. Carbon nanodots as a matrix for the analysis of low-molecular-weight molecules in both positive- and negative-ion matrix-assisted laser desorption/ionization time-of-flight mass spectrometry and quantification of glucose and uric acid in real samples. Chem. 2013, 85, 6646–6652, doi:10.1021/ac401601r.

17. Xu, S.; Li, Y.; Zou, H.; Qiu, J.; Guo, Z.; Guo, B. Carbon nanotubes as assisted matrix for laser desorption/ionization time-of-flight mass spectrometry. Chem. 2003, 75, 6191–6195, doi:10.1021/ac0345695.

18. Tang, H.W.; Ng, K.M.; Lu, W.; Che, C.M. Ion desorption efficiency and internal energy transfer in carbon-based surface-assisted laser desorption/ionization mass spectrometry: Desorption mechanism(s) and the design of SALDI substrates. Chem. 2009, 81, 4720–4729, doi:10.1021/ac8026367.

19. Lu, ; Yang, X.; Yang, Y.; Qin, P.; Wu, X.; Cai, Z. Nanomaterials as assisted matrix of laser desorption/ionization time-of-flight mass spectrometry for the analysis of small molecules. Nanomaterials 2017, 7, 87, doi:10.3390/nano7040087.

20. Liu, Q.; Cheng, M.; Jiang, G. Mildly oxidized graphene: Facile synthesis, characterization, and application as a matrix in MALDI mass spectrometry. Eur. J. 2013, 19, 5561–5565, doi:10.1002/chem.201203791.

21. Kim, Y.K.; Min, D.H. Mechanistic study of laser desorption/ionization of small molecules on graphene oxide multilayer films. Langmuir 2014, 30, 12675–12683, doi:10.1021/la5027653.

22. Wei, J.; Buriak, J.M.; Siuzdak, G. Desorption-ionization mass spectrometry on porous silicon. Nature 1999, 399, 243–246, doi:10.1038/20400.

23. Nakamura, Y.; Soejima, T. TiO2 Nanocoral structures as versatile substrates for surface-assisted laser desorption/ionization mass spectrometry. ChemNanoMat 2019, 5, 447–455, doi:10.1002/cnma.201800588.

24. Lewis, W.G.; Shen, Z.; Finn, M.G.; Siuzdak, G. Desorption/ionization on silicon (DIOS) mass spectrometry: Background and applications. J. Mass Spectrom. 2003, 226, 107–116, doi:10.1016/S1387-3806(02)00973-9.

25. Thomas, J.J.; Shen, Z.; Crowell, J.E.; Finn, M.G.; Siuzdak, G. Desorption/ionization on silicon (DIOS): A diverse mass spectrometry platform for protein characterization. Natl. Acad. Sci. USA 2001, 98, 4932–4937, doi:10.1073/pnas.081069298.

26. Sweetman, M.J.; Mclnnes, S.J.P.; Vasani, R.B.; Guinan, T.; Blencowe, A.; Voelcker, N.H. Rapid, metal-free hydrosilanisation chemistry for porous silicon surface modification. Commun. 2015, 51, 10640,

doi:10.1039/c5cc02689j.

27. Luo, G.; Chen, Y.; Siuzdak, G.; Vertes, A. Surface modification and laser pulse length effects on internal energy transfer in DIOS. Phys. Chem. B 2005, 109, 24450–24456, doi:10.1021/jp054311d.

28. Wang, X.N.; Tang, W.; Gordon, A.; Wang, H.Y.; Xu, L.; Li, P.; Li, B. Porous TiO2 film immobilized with gold nanoparticles for dual-polarity SALDI MS detection and imaging ACS Appl. Mater. Interfaces 2020, 12, 42567–42575, doi:10.1021/acsami.0c12949.

29. Zhu, ; Teng, F.; Wang, Z.; Wang, Y.; Lu, N. Superhydrophobic glass substrates coated with fluorosilane-coated silica nanoparticles and silver nanoparticles for surface-assisted laser desorption/ionization mass spectrometry. ACS Appl. Nano Mater. 2019, 2, 3813–3818, doi:10.1021/acsanm.9b00688.

30. Min, ; Zhang, X.; Chen, X.; Li, S.; Zhu, J.J. N-Doped graphene: An alternative carbon-based matrix for highly efficient detection of small molecules by negative ion MALDI-TOF-MS. Anal. Chem. 2014, 86, 9122–9130, doi:10.1021/ac501943n.

31. Huang, X.; Liu, Q.; Huang, X.; Nie, Z.; Ruan, T.; Du, Y.; Jiang, G. Fluorographene as a mass spectrometry probe for high-throughput identification and screening of emerging chemical contaminants in complex samples. Chem. 2017, 89, 1307–1314, doi:10.1021/acs.analchem.6b04167.

32. Zhao, ; Li, Y.; Wang, J.; Cheng, M.; Zhao, Z.; Zhang, H.; Wang, C.; Wang, J.; Qiao, Y.; Wang, J. Dual-Ion-Mode MALDI MS Detection of small molecules with the O-P,N-Doped carbon/graphene matrix. ACS Appl. Mater. Interfaces 2018, 10, 37732–37742, doi:10.1021/acsami.8b14643.

33. Wang, ; Jiamg, X.; Li, J.; He, B.; Liu, Q.; Hu, L.; Jiang, G. 3D printing of graphene-doped target for "matrix-free" laser desorption/ionization mass spectrometry. Chem. Commun. 2018, 54, 2723–2726, doi:10.1039/c7cc09649f.

34. Huang, ; Liu, Q.; Fu, J.; Nie, Z.; Gao, K.; Jiang, G. Screening of toxic chemicals in a single drop of human whole blood using ordered mesoporous carbon as a mass spectrometry probe. Anal. Chem. 2016, 88, 4107–4113, doi:10.1021/acs.analchem.6b00444.

35. Zhou, D.; Guo, S.; Zhang, M.; Liu, Y.; Chen, T.; Li, Z. Mass spectrometry imaging of small molecules in biological tissues using graphene oxide as a matrix. Chim. Acta 2017, 962, 52–59, doi:10.1016/j.aca.2017.01.043.

36. Shi, ; Deng, C.; Zhang, X.; Yang, P. Synthesis of highly water-dispersible polydopamine-modified multiwalled carbon nanotubes for matrix-assisted laser desorption/ionization mass spectrometry analysis. ACS Appl. Mater. Interfaces 2013, 5, 7770–7776, doi:10.1021/am4024143.

37. Lu, W.; Li, Y.; Li, R.; Shuang, S.; Dong, C.; Cai, Z. Facile synthesis of N-Doped Carbon dots as a new matrix for detection of hydroxy-polycyclic aromatic hydrocarbons by negative-ion matrix-assisted laser desorption/ionization time-of-flight mass spectrometry. ACS Appl. Mater. Interfaces 2016, 8, 12976–12984, doi:10.1021/acsami.6b01510.

38. Han, ; Li, S.; Peng, Z.; Al-Yuobi, A.O.; Bashammakh, A.S.O.; El-Shahawi, M.S.; Leblanc, R.M. Interactions between carbon nanomaterials and biomolecules. J. Oleo Sci. 2016, 65, 1–7, doi:10.5650/jos.ess15248.

39. Perreault, F.; Fonseca De Faria, A.; Elimelech, M. Environmental applications of graphene-based nanomaterials. Soc. Rev. 2015, 44, 5861–5896, doi:10.1039/c5cs00021a.

40. Yu, S.; Wang, X.; Yao, W.; Wang, J.; Ji, Y.; Ai, Y.; Alsaedi, A.; Hayat, T.; Wang, X. Macroscopic, spectroscopic, and theoretical investigation for the interaction of phenol and naphthol on reduced graphene oxide. Sci. Technol. 2017, 51, 3278–3286, doi:10.1021/acs.est.6b06259.

41. Yu, Y.; Murthy, B.N.; Shapter, J.G.; Constantopoulos, K.T.; Voelcker, N.H.; Ellis, A.V. Benzene carboxylic acid derivatized graphene oxide nanosheets on natural zeolites as effective adsorbents for cationic dye removal. Hazard. Mater. 2013, 260, 330–338, doi:10.1016/j.jhazmat.2013.05.041.

42. Claramunt, S.; Varea, A.; López-Díaz, D.; Velázquez, M.M.; Cornet, A.; Cirera, A. The importance of interbands on the interpretation of the Raman spectrum of graphene oxide. Phys. Chem. C 2015, 119, 10123–10129, doi:10.1021/acs.jpcc.5b01590.

43. Cançado, L.G.; Jorio, A.; Martins Ferreira, E.H.; Stavale, F.; Achete, C.A.; Capaz, R.B.; Moutinho, M.V.O.; Lombardo, A.; Kulmala, T.S.; Ferrari, A.C. Quantifying Defects in Graphene via Raman Spectroscopy at Different Excitation Energies. Nano Lett. 2011, 11, 3190–3196, doi:10.1021/nl201432g.

44. Gómez, J.; Villaro, E.; Navas, A.; Recio, I. Testing the influence of the temperature, RH and filler type and content on the universal power law for new reduced graphene oxide TPU composites. Res. Express 2017, 4, 105020, doi:10.1088/2053-1591/aa8e11.

45. Dave, H.; Gong, C.; Robertson, A.W.; Warner, J.H.; Grossman, J.C. Chemistry and structure of graphene oxide via direct imaging. ACS Nano 2016, 10, 7515–7522, doi:10.1021/acsnano.6b02391.

46. Dreyer, D.R.; Park, ; Bielawski, C.W.; Ruoff, R.S. The chemistry of graphene oxide. Chem. Soc. Rev. 2010, 39, 228–240, doi:10.1039/B917103G.

47. Shojaeenezhad, S.S.; Farbod, M.; Kazeminezhad, I. Effects of initial graphite particle size and shape on oxidation time in graphene oxide prepared by Hummers' method. Sci. Adv. Mater. Devices 2017, 2, 470–475, doi:10.1016/j.jsamd.2017.09.003.

48. Mouhat, ; Coudert, F.; Bocquet, M. Structure and chemistry of graphene oxide in liquid water from first principles. Nat. Commun. 2020, 11, 1566, doi:10.1038/s41467-020-15381-y.

49. Brisebois, P.P.; Siaj, M. Harvesting Graphene Oxide-Years: 1859 to 2019 A Review of its Structure, Synthesis, Properties and Exfoliation. Mater. Chem. C 2020, 8, 1517–1547, doi:10.1039/C9TC03251G.

50. Chen, D.; Feng, H.; Li, J. Graphene Oxide: Preparation, functionalization, and electrochemical applications. Rev. 2012, 112, 6027–6053, doi:10.1021/cr300115g.

51. Loh, K.P.; Bao, Q.; Eda, G.; Chhowalla, M. Graphene oxide as a chemically tunable platform for optical applications. Chem. 2010, 2, 1015–1024, doi:10.1038/nchem.907.

52. Guex, L.G.; Sacchi, B.; Peuvot, K.F.; Andersson, R.L.; Pourrahimi, A.M.; Ström, ; Farris, S.; Olsson, R.T. Experimental review: Chemical reduction of graphene oxide (GO) to reduced graphene oxide (rGO) by aqueous chemistry. Nanoscale 2017, 9, 9562, doi:10.1039/c7nr02943h.

53. Zhang, J.; Zheng, X.; Ni, Y. Selective enrichment and MALDI-TOF MS analysis of small molecule compounds with vicinal diols by boric acid-functionalized graphene oxide. Am. Soc. Mass Spectrom. 2015, 26, 1291–1298, doi:10.1007/s13361-015-1162-6.

54. Jiang, B.; Qu, Y.; Zhang, L.; Liang, Z.; Zhang, Y. 4-Mercaptophenylboronic acid functionalized graphene oxide composites: Preparation, characterization and selective enrichment of glycopeptides. Chim. Acta 2016, 912, 41–48, doi:10.1016/j.aca.2016.01.018.

55. Tang, L.A.L.; Wang, J.; Loh, K.P. Graphene-based SELDI probe with ultrahigh extraction and sensitivity for DNA oligomer. Am. Chem. Soc. 2010, 132, 10976–10977, doi:10.1021/ja104017y.

56. Li, J.Y.; Long, X.Y.; Sheng, D.; Lian, H.Z. Organic molecule-assisted synthesis of Fe3O4/graphene oxide nanocomposites for selective capture of low-abundance peptides and phosphopeptides. Talanta 2020, 208, 120437, doi:10.1016/j.talanta.2019.120437.

57. Dong, X.; Cheng, J.; Li, J.; Wang, Y. Graphene as a novel matrix for the analysis of small molecules by MALDI-TOF MS. Chem. 2010, 82, 6208–6214, doi:10.1021/ac101022m.

58. Bøggild, P. The war on fake Nature 2018, 562, 502–503, doi:10.1038/d41586-018-06939-4.

59. Georgakilas, V.; Perman, J.A.; Tucek, J.; Zboril, R. Broad family of carbon nanoallotropes: Classification, chemistry, and applications of fullerenes, carbon dots, nanotubes, graphene, nanodiamonds, and combined superstructures. Rev. 2015, 115, 4744–4822, doi:10.1021/cr500304f.

60. Chang, H.; Tang, L.; Wang, Y.; Jiang, J.; Li, J. Graphene fluorescence resonance energy transfer aptasensor for the thrombin detection. Chem. 2010, 82, 2341–2346, doi:10.1021/ac9025384.

61. Zhou, X.; Wei, Y.; He, Q.; Boey, F.; Zhang, Q.; Zhang, H. Reduced graphene oxide films used as matrix of MALDI-TOF-MS for detection of octachlorodibenzo-p-dioxin. Commun. 2010, 46, 6974–6976, doi:10.1039/c0cc01681k.

62. Lu, M.; Lai, Y.; Chen, G.; Cai, Z. Matrix interference-free method for the analysis of small molecules by using negative ion laser desorption/ionization on graphene flakes. Chem. 2011, 83, 3161–3169, doi:10.1021/ac2002559.

63. Liu, C.W.; Chien, M.W.; Su, C.Y.; Chen, H.Y.; Li, L.J.; Lai, C.C. Analysis of flavonoids by graphene-based surface-assisted laser desorption/ionization time-of-flight mass spectrometry. Analyst 2012, 137, 5809–5816, doi:10.1039/c2an36155h.

64. Kim, Y.K.; Min, D.H. The structural influence of graphene oxide on its fragmentation during laser desorption/ionization mass spectrometry for efficient small-molecule analysis. Eur. J. 2015, 21, 1–8, doi:10.1002/chem.201404067.

65. Li, Z.; Zhang, W.; Luo, Y.; Yang, J.; Hou, J.G. How graphene is cut upon oxidation? Am. Chem. Soc. 2009, 131, 6320–6321, doi:10.1021/ja8094729.

66. Hong, Y.L.; Lee, J.; Ku, B.C.; Kang, K.; Lee, S.; Ryu, S.; Kim, Y.K. The influence of oxidative debris on the fragmentation and laser desorption/ionization process of graphene oxide derivatives. New J. Chem. 2018, 42, 12692–12697, doi:10.1039/c8nj02628a.

67. Hong, Y.L.; Seo, T.H.; Jang, H.J.; Kim, Y.K. The effect of oxidative debris on the laser desorption/ionization efficiency of graphene oxide derivates for mass spectrometric analysis of small molecules and synthetic polymers. Sci. 2019, 35, 1097–1102, doi:10.2116/analsci.19P205.

68. Rourke, J.P.; Pandey, P.A.; Moore, J.J.; Bates, M.; Kinloch, I.A.; Young, R.J.; Wilson, N.R. The real graphene oxide revealed: Stripping the oxidative debris from the graphene-like sheets. Angew. Chem. 2011, 50, 3173–3177.